Springer

KSME

Journal of Mechanical Science and Technology 25 (6) (2011) 1543~1550
www.springerlink.com/content/1738-494x
DOI 10.1007/s12206-011-0408-x

Evaluation of weldability for resistance spot welded single-lap joint between GA780DP and hot-stamped 22MnB5 steel sheets †

Hong-Seok Choi[1], Geun-Hwan Park[1], Woo-Seung Lim[1] and Byung-min Kim[2,*]

[1]*Precision Manufacturing and Systems Division, Pusan National University, Busan, 609-735, Korea*
[2]*School of Mechanical Engineering, Pusan National University, Busan, 609-735, Korea*

(Manuscript Received October 4, 2010; Revised February 10, 2011; Accepted March 6, 2011)

Abstract

Recently, in the automotive industry, Al-coated boron steel sheets (22MnB5) have been used for hot stamping, and the use of these sheets makes it possible to achieve a tensile strength of over 1,500 MPa, since a metallurgical transformation from austenite to martensite occurs during the process. In this study, resistance spot welding (RSW) experiments were performed in order to evaluate the weldability of single-lap joints between GA780DP and 22MnB5. The effect of the weld current on the nugget diameter and load-carrying capacity was evaluated by observing the nugget diameter and performing a tensile-shear test. Furthermore, the fracture behavior was evaluated by carrying out optical microscopy, scanning electron microscopy (SEM), and energy-dispersive X-ray spectroscopy (EDX) observations. Ductile regions were observed on the interfacially fractured surface of the weld, and this implies that a high load-carrying capacity can be obtained even when interfacial fracture (IF) occurs. IF is caused by the stress concentration resulting from the presence of the sharp notch at the boundary of the nugget as well as by the high hardness and the brittle microstructure of the weld; the microstructure is brittle because of the high carbon equivalent (C_{eq}) and the penetration of Al in the weld.

Keywords: 22MnB5; GA780DP; Aluminum coated layer; Hot stamping; Interfacial fracture; Resistance spot welding; Single lap joint; Tensile-shear strength

1. Introduction

The Ultra-high-strength steel (UHSS) steets, such as dual-phase (DP), transformation induced plasticity (TRIP), and complex phase (CP) steel, whose tensile strengths range from 780 MPa to 980 MPa, have been used in Body-in-White (BIW) in order to reduce the weight and enhance the safety of automobiles [1]. However, these types of UHSS also have drawbacks such as limited formability, which causes fracture and severe springback during forming at room temperature [2, 3].

In order to increase strength and to solve the abovementioned problems, the hot stamping process involving the use of boron manganese alloy steel (22MnB5) has been developed. In the hot stamping process, a blank is heated to between 900 and 950°C and is then rapidly transferred to the press where the whole deforming phase should proceed in the fully austenitic condition; the use of cooled dies guarantees rapid cooling of the sheet during the process, and thus, a martensitic microstructure with a tensile strength of over 1,500 MPa is obtained through a phase transformation [4, 5]. Hot-stamped components have been used in crash-relevant parts such as bumpers, pillars, roof rails, and impact beams.

On the other hand, one of the important parameters before applying this process and material to the automotive components is resistance spot weldability of used high strength material. In particular, it is known that interfacial fracture (IF), which is considered to be a failure in the weld of mild steel, is easily caused by hard and brittle martensite, which is formed in the weld because of the high carbon equivalent (C_{eq}) [6, 7]. Although research on double impulse, post weld, and temper control has been conducted in order to solve this problem, these methods have restricted applicability in industrial fields [8, 9].

Park et al. asserted that the acceptable welding region of high strength steel is narrow because of the expulsion that occurs in the range of high weld currents [7]. On the other hand, the Al-coated 22MnB5 contains a large amount of alloying elements such as Mn and Cr; this results in an increase in C_{eq}, and the tensile strength after hot stamping increases to over 1,500 MPa. Consequently, it is obvious that the welding condition for 22MnB5 is different from that for conventional high-strength steel to prevent expulsion as well as to obtain the required strength. Furthermore, Lee et al. investigated the

† This paper was recommended for publication in revised form by Editor Dae-Eun Kim

* Corresponding author. Tel.: +82 51 510 3074, Fax.: +82 51 581 3075
E-mail address: bmkim@pusan.ac.kr

Table 1. Chemical compositions of the two steels used.

Material	C	Si	Mn	Cr	P	S	B	Fe	C_{eq}
22MnB5	0.22	0.4	1.4	0.37	0.03	0.015	0.003	Bal	0.54
GA780DP	0.07	1.0	2.5	0.1	Mo	V	Ni		0.56
					0.02	0.01	0.08		

C_{eq} = C+Mn/6+Si/24+Cr/5+(Ni+Cu)/15

effect of the boron content in high-strength steel on weldability and reported that the amount of boron influences the occurrence of cracks in the weld [10].

In order to prevent oxidation during heating and transfer, an Al coating is deposited on 22MnB5 with amount of 140g/m^2 (thickness: 30 μm). Cha et al. investigated the weldability of Al-coated mild steel sheet. They asserted that the appropriate welding conditions for Al-coated steel differ from those for uncoated steel because of the differences between the electrical conductivities and melting points of the coated layer and the substrate [11].

In this study, RSW experiment of single lap joint between 22MnB5 and GA780DP is performed in order to evaluate weldability. For this, the effect of the weld current on the nugget diameter and load-carrying capacity was evaluated by observing the nugget diameter and performing a tensile-shear test. Furthurmore, the fractured surface was observed in order to evaluate fracture behavior of the weld between 22MnB5 and GA780DP steel sheets.

2. Test materials

The materials selected in this study were 22MnB5 after hot stamping and GA780DP steel sheets. The thicknesses of used steel sheets are 1.6 mm and 2.0 mm, respectively. Table 1 shows the chemical composition and C_{eq} of the two steels. The high C_{eq} of these materials implies that a hard and brittle martensite microstructure is formed in the weld zone. Due to the cracking susceptibility, this will readily lead to crack and propagation under the loading condition if C_{eq} is greater than 0.24 [12].

Figs. 1(a) and (b) show the microstructure of 22MnB5 as-received and after hot stamping, respectively. The microstructure of as-received 22MnB5 is composed of hypoeutectoid ferrite and a small amount of pearlite, and is transformed to lath martensite after hot stamping due to the formation of an interstitial solid solution of carbon and boron [13]. On the other hand, the 22MnB5 has an Al coating, and an intermetallic compound layer (IMC) of Fe_2Al_5 resulting from diffusion during the hot dipping process is formed between the coated layer and the substrate. After hot stamping, an oxidation layer with small cracks in the Al-coated layer is observed, and the IMC layer also increases by over 10 μm due to diffusion between the coated layer and the substrate during hot stamping [14].

Table 2 shows the mechanical properties of 22MnB5 and GA780DP. The tensile strength of 22MnB5 is approximately

Table 2. Mechanical properties of 22MnB5 and GA780DP.

Material	YS (MPa)	UTS (MPa)	Elongation (%)	Hardness (Hmv)	Remark
22MnB5	415	580	28.4	190	As-received
	1,132	1,480	6.5	540	After hot stamping
GA780DP	484	792	13.2	250	As-received

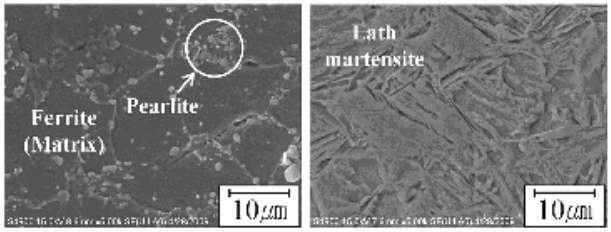

(a) Substrate; as received (left), after hot stamping (right)

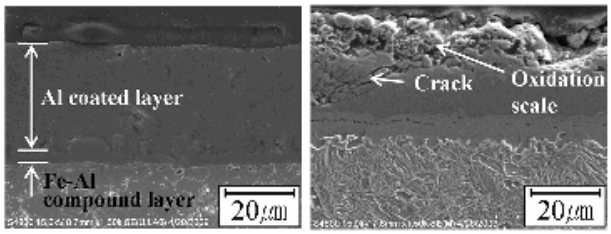

(b) Coated layer; as received (left), after hot stamping (right)

Fig. 1. Microstructure of the 22MnB5 used in hot stamping.

1,500 MPa, whereas that of the as-received material of 600 MPa. Therefore, the required weld strength should be increased in order to meet the quality of weld requirements according to the improved mechanical properties.

3. Experimental procedures

Resistance spot welding (RSW) was performed using a specimen of length 125 mm and width 40 mm, according to KS B 0851 of the Korean Standards Association [15]. Prior to the RSW experiment, 22MnB5 was heated to 900°C for 5 minutes and quenched between cooled dies in order to obtain the martensite microstructure, similarly to the hot stamping process. The specimens were cleaned using an ultrasonic washer to eliminate oils and impurities. RSW experiments were performed using a single-phase resistance spot welder (PH4-1078) and electrodes with Cr-Cu alloy flat-tip ends of 6.0 mm diameter. Coolant was supplied to the electrodes at a rate of 10 liters per minute during RSW. Four sets of RSW experiments were performed at one weld condition to evaluate the nugget diameter and to obtain the average tensile-shear strength for three sets.

In order to evaluate the nugget diameter accurately, spot welds were cross-sectioned, mounted, polished with carbide paper and diamond paste, and finally etched with 5% nital reagent. The microstructures were observed using optical microscopy, scanning electron microscopy (SEM) and energy-

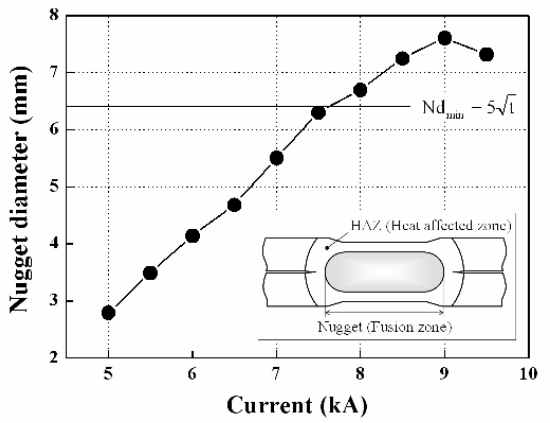

Fig. 2. Nugget diameter according to the weld current under an electrode force of 6 kN and weld time of 20 cycle.

dispersive X-ray spectroscopy (EDX) including mapping were implemented to investigate the microstructure and the fractured surface of the welds in detail. Microhardness measurements were taken at intervals of 0.2 mm using a microvickers hardness tester (MXT-α) at an applied load of 500 g and a dwelling time of 10 s. Tensile-shear tests were performed at a low crosshead velocity of 1 mm/min.

4. Results and discussions

4.1 Effect of weld current

The weld current is one of the important factors in RSW, and resistance heat for the formation of the weld nugget is proportional to the square of the current, as presented in Eq. (1).

$$Q(J) = I^2Rt \quad (1)$$

In general, the quality and strength of a weld is evaluated by the size of the weld nugget [6]. Fig. 2 shows the nugget diameter according to the weld current at an electrode force of 6 kN and a weld time of 20 cycle. It is clearly observed that the nugget diameter increases with increasing weld current. It is known that the strength of the weld is sufficient when the minimum nugget diameter (N_{dmin}) is over $5\sqrt{T}$ (mm) according to KS B 0850 [16], where T is the thickness of the thinner of the two sheets. Consequently, N_{dmin} is calculated to be 6.32 mm on the basis of 22MnB5 having a thickness of 1.6 mm, and this condition is met at a weld current of over 8 kA. However, large voids located at the center of the weld nugget along the solidification parting line, which result from expulsion and solidification shrinkage, are observed in the weld at a current of 9.5 kA, as seen in Fig. 3. Therefore, it is confirmed that the appropriate weld current is between 8 and 9 kA.

A tensile-shear test is performed in order to evaluate the effect of the weld current on the strength and load-carrying capacity. Fig. 4 shows the peak load for the spot welds as a function of weld current while other parameters are kept constant.

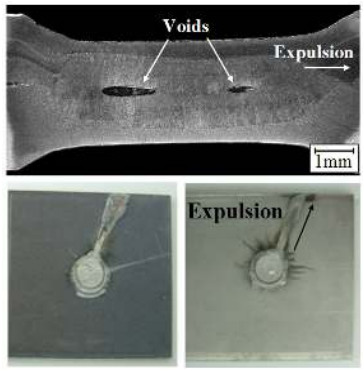

Fig. 3. Weld nugget under a current of 9.5 kA, electrode force of 6 kN and weld time of 20 cycle.

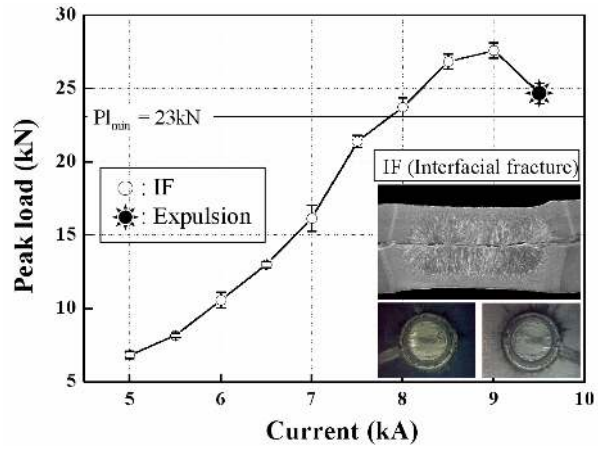

Fig. 4. Peak load according to the weld current under an electrode force of 6 kN and weld time of 20 cycle.

Each data point represents an average of three specimens. It is seen that the peak load increases with increasing weld current. This is because nugget diameter, which increases load-carrying capacity, is increased by the weld current.

In accordance with KS B 0850, the required peak load, based on 22MnB5 with tensile stress of 1,500 MPa and a thickness of 1.6 mm, is 23 kN [16]. Consequently, the appropriate weld current must be at least 8 kA in order to satisfy the prescribed peak load. The maximum fracture load is reached for a weld current of 9 kA, while the failure mode is just interfacial fracture, which is considered unacceptable for mild steel.

On the other hand, it is observed that the peak load of the weld performed under a current of 9.5 kA decreases slightly as marked on the plot. This is because expulsion resulting from excessive heat input to the nugget occurs at the interface between two sheets. Expulsion leads to a decrease in nugget volume as well as an increase in shrinkage and solidification cracks, which decreases the static load-carrying capacity [17].

4.2 Microstructural change in the weld

SEM observation was used to examine the microstructural changes as shown in Fig. 6. Fig. 6(b) shows the microstructure

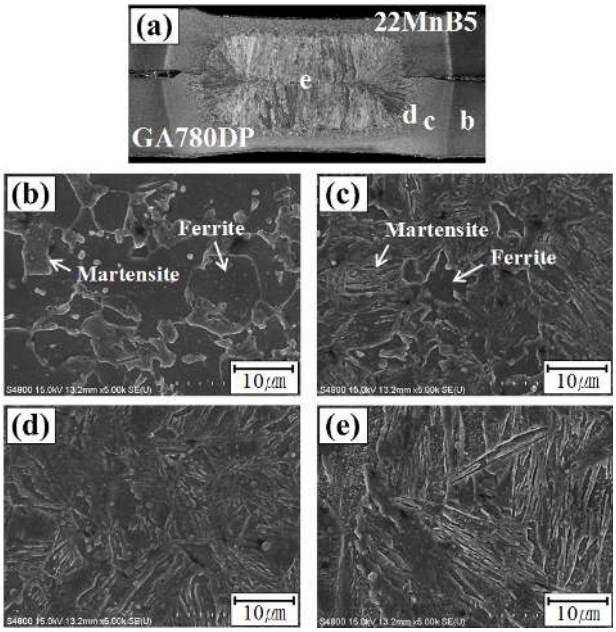

Fig. 5. Microstructural change from the base metal to the weld nugget on the GA780DP side (a) Weld nugget where the location of micrographs (b-e) is indicated by b-e; (b) base metal; (c) transition zone between base metal and HAZ; (d) HAZ close to fusion zone; (e) fusion zone.

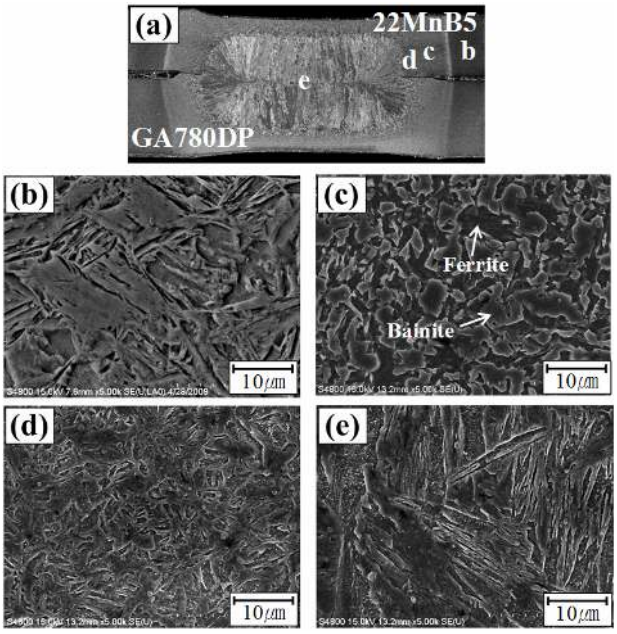

Fig. 6. Microstructural change from the base metal to the weld nugget on the 22MnB5 side (a) Weld nugget where the location of micrographs (b-e) is indicated by b-e; (b) base metal; (c) transition zone between base metal and HAZ; (d) HAZ close to fusion zone; (e) fusion zone.

of the base metal, GA780DP, which is composed of a martensite and ferrite matrix. It is known that the martensite volume fraction increases gradually in the heat-affected zone (HAZ) near the base metal, as seen in Fig. 5(c). On the other hand, the amount of martensite that is finer than that in the fusion zone

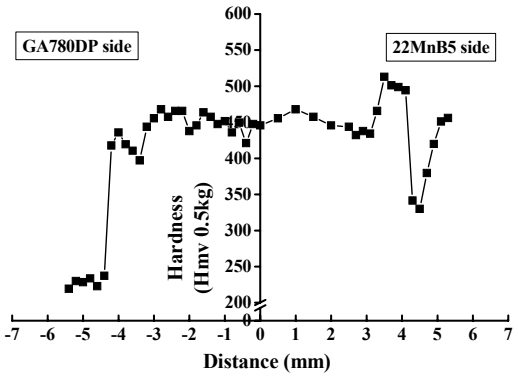

Fig. 7. Typical hardness profile between GA780DP and 22MnB5 after RSW with 8 kA, 6 kN and 20 cycles.

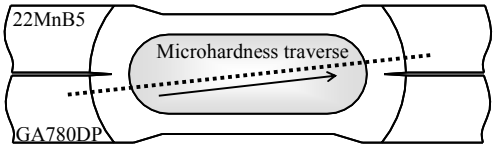

Fig. 8. Schematic of microhardness traverse.

(Fig. 5(e)) increases, as shown in Fig. 5(d). This phenomenon is explained by the fact that, because austenization is incomplete in the HAZ even when austenite grains have formed, grain growth is restricted by the formation of martensite and thermal cycles [17]. Whereas the grains are fine in the HAZ, the resulting high density of the grain boundaries constitutes an obstacle to the formation of large martensite.

Fig. 6 shows the microstructural change in the weld nugget on the 22MnB5 side. As seen in Fig. 6(b), bainite is observed in the ferrite matrix. This microstructure results from the annealing effect by the relatively slow cooling rate at the HAZ near the base metal [18]. On the other hand, quite fine martensite is observed in the HAZ near the fusion zone, as shown in Fig. 6(c). These microstructural transformations affect the hardness distribution in the weld.

4.3 Hardness profile

Fig. 7 shows a microhardness profile of the weld between 22MnB5 and GA780DP. The hardness was measured on the two stack-up spot welding sample as presented in Fig. 8, and obtained at 0.2 mm intervals. Based on GA780DP, the hardness of the weld nugget increases up to around Hmv 450, which is about twice that of the base metal. This is due to the fact that alloying contents such as chromium and manganese, increasing the carbon equivalent, are contained in GA780DP [12]. Furthermore, the high cooling rate during RSW leads to the formation of hard and brittle martensite in the weld zone. In addition, there is a noticeable drop in the HAZ away from the fusion zone root. According to other researchers, this softening is caused by tempered martensite in that region [19].

Conversely, a significant decrease in the hardness to Hmv 320 clearly appears in the HAZ, compared with the hardness

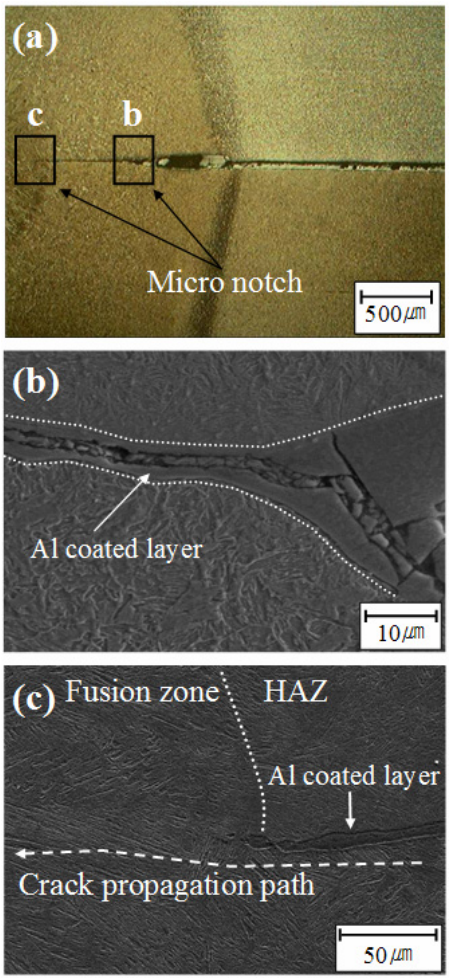

Fig. 9. Optical image (OM) and SEM image of weld nugget (a) Optical image of the cross-section of nugget-surrounding area; (b) magnified views of region 'b'; (c) magnified view of region 'c'.

of the base metal and fusion zone. This is because the martensite of 22MnB5 after RSW is transformed to soft bainite in the pre-eutectoid ferrite matrix by the annealing effect, as shown in Fig. 7(c). The highest hardness of over Hmv 500 is observed in the HAZ close to the fusion zone. This is reported due to the formation of MC carbide resulting from the diffusion of chromium, which has a strong affinity with carbon [18]. However, this is not observed clearly in the microstructure. It is thought simply that the finer martensite in the HAZ contributes to the highest hardness throughout the weld.

4.4 Examination of interfacial fracture

Interfacial fracture occurs in all weld specimens under the considered weld conditions. Fig. 9 shows optical microscopy and SEM images of the nugget-surrounding area. As seen in Fig. 9(a), a sharp notch is observed in the edge of nugget. Cracks would initiate from the edge due to the stress concentration resulting from the sharp notch [12]. Fig. 9(b) shows a magnified image of region 'b'. It is known that the boundary

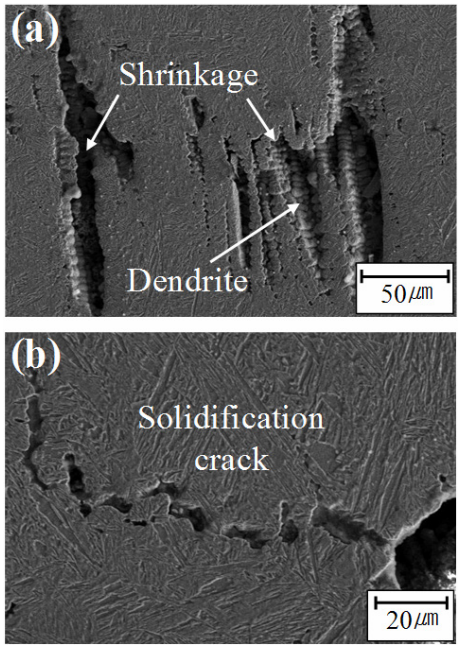

Fig. 10. Magnified image of the fusion zone (a) Shrinkage and dendrite structure; (b) solidification crack.

of the weld nugget near the faying surfaces is weakly bonded and relatively brittle due to the molten Al coating. This Al-coated layer is also observed over the fusion zone, which tends to crack during loading. Consequently, cracks initiated from the sharp notch would penetrate through the weakly bonded region and propagate across the fusion zone. This phenomenon is one of the reasons for the occurrence of interfacial fracture in the weld of 22MnB5 and GA780DP.

Fig. 10 shows a magnified image of the fusion zone at a cross-sectioned nugget. Shrinkage (Fig. 10(a)) and solidification cracks (Fig. 10(b)) are clearly observed in the nugget, which would cause the occurrence of interfacial fracture and decrease the weld properties [12, 17].

In order to examine the interfacial fracture in detail, the fractured surface was observed by SEM and EDX. Fig. 11 shows SEM images of the interfacially fractured surface. Fig. 11(a) shows an overall view of the fractured weld zone at a low magnification. It is known that solidification cracks and shrinkages that are observed at the cross-sectioned nugget (as seen in Fig. 10) appear on the failed surface. These minute features can be seen in Fig. 11(b) at a higher magnification. More detailed images of shrinkages and cracks are shown in Figs. 11(c), (d) and (e). Dendrite structures are clearly observed at a higher magnification as seen in Fig. 11(d). This is direct evidence of the defects caused by the shrinkage and solidification cracks. These would cause interfacial fracture and decrease the weld properties.

According to Marya et al. the higher carbon equivalent makes the weld hard and brittle, which congregated in the grain boundaries and increased the boundary energy to easily cause the solidification cracks [17]. The carbon equivalents of

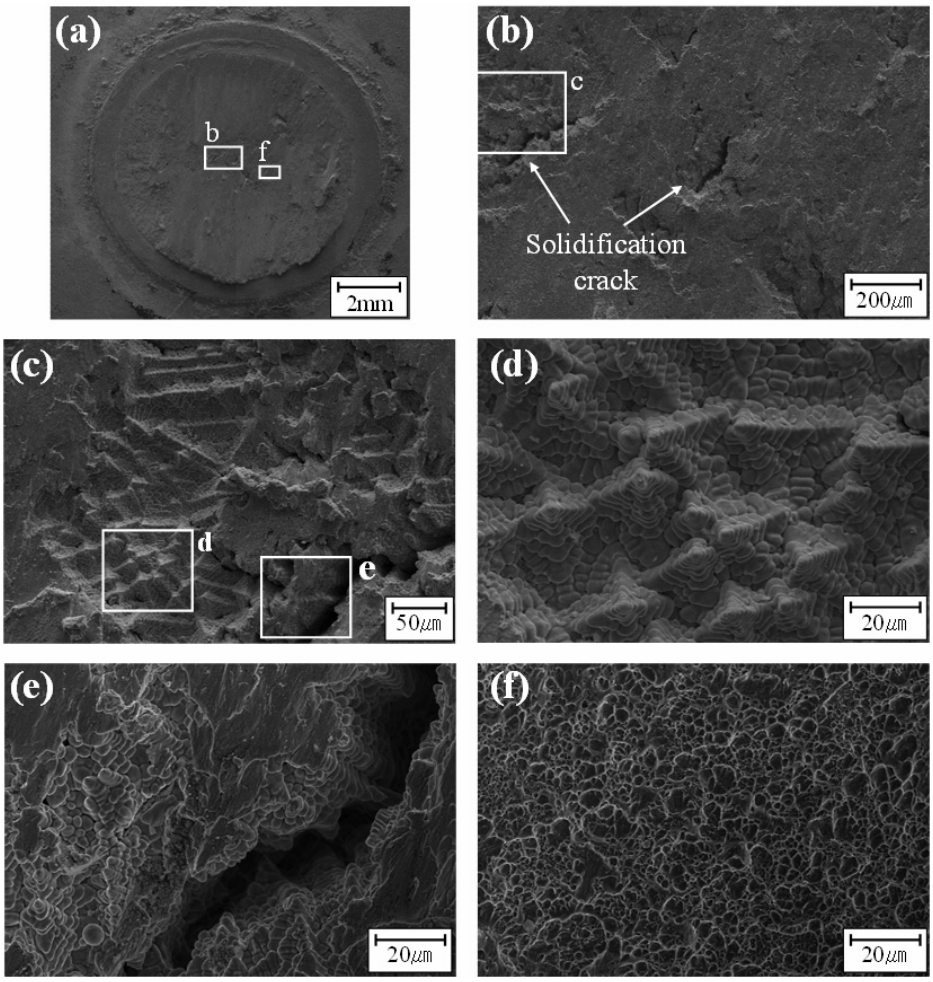

Fig. 11. SEM images of the fractured weld zone (a) Overall view of the fractured weld zone; (b) and (c) higher magnification view of the weld; (d) dendrites; (e) magnified image of solidification crack and shrinkage; (f) ductile fracture characteristics (dimple).

the materials studied, 22MnB5 and GA780DP, are 0.54 and 0.56, respectively. The weld will fail interfacially if the carbon equivalent is greater than 0.24.

On the other hand, the reason for the high strength in the specimen welded under high current conditions is thought to be the ductile microstructure that appears throughout the fractured surface (see Fig. 11(f)) even though interfacial fracture has occurred.

Fig. 12 shows EDX and mapping analysis results of the fractured zone. As seen in Fig. 12(b), the interfacially fractured area contains Al at the nugget and surrounding region. As detailed in Figs. 12(c) and (d), Al is clearly observed in that region. The Al content in the weld would exist either as a solid solution or in alloying elements such as Fe_2Al_5 and FeAl, which exhibit hard and brittle properties. These alloyed elements influence interfacial fracture during load carrying.

5. Conclusions

The resistance spot weldability between 22MnB5, which is increasingly being used in hot stamping for reducing the weight of automobiles and for improving crashworthiness, and GA780DP steel sheets was investigated in this study. On the basis of the experimental results, the following conclusions can be drawn:

(1) The nugget diameter increases with increasing weld current. The required nugget diameter can be obtained at weld currents greater than 8 kA. However, the nugget diameter decreases slightly at a current of 9.5 kA because of expulsion at the faying surface.

(2) The results of a tensile-shear test show that the required strength is achieved at a current of over 8 kA, and the maximum value is achieved at 9 kA. It is believed that the increase in the load-carrying capacity with increasing weld current results from the increase in the nugget diameter. The peak load of the specimen welded at a current of 9.5 kA was lower; this sample undergoes expulsion, which results in a decrease in the nugget volume.

(3) Significant difference of hardness is observed at heat affected zone of 22MnB5. The hardness in the HAZ near the fusion zone is higher than that of the base metal because of the fine martensite. Moreover, the presence of ferrite and bainite

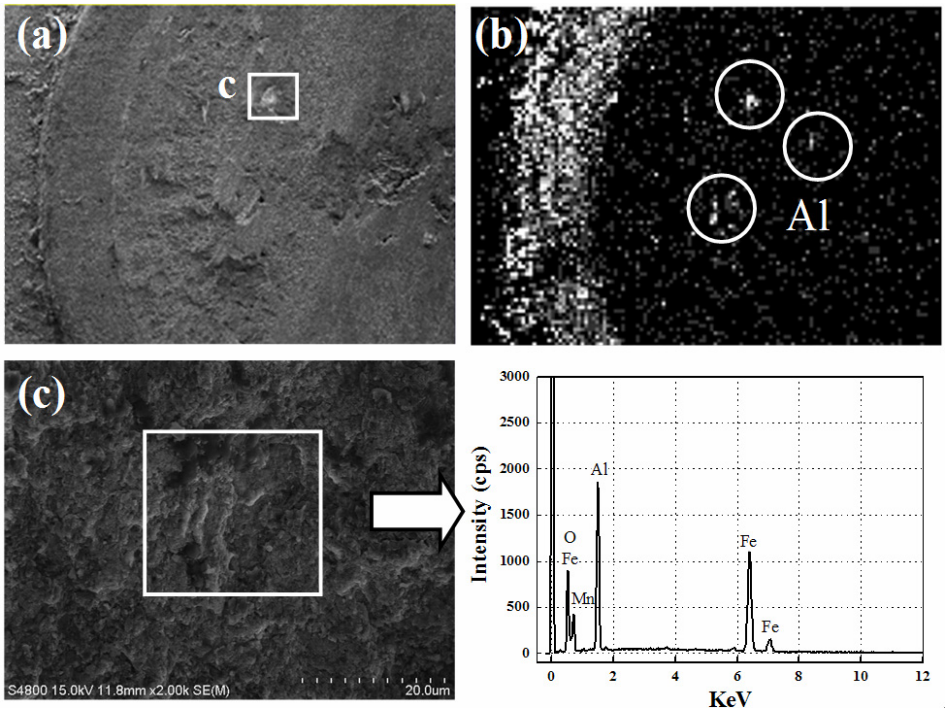

Fig. 12. EDX and mapping results of the fractured zone (a) SEM image of fractured surface; (b) mapping result of fractured zone; white indicates that Al content is detected; (c) magnified view of region 'c' and EDX analysis result.

microstructures, which leads to a decrease in hardness, is observed in the HAZ close to the base metal. The occurrence of these ductile structures is due to the phase transformation caused by different cooling rate during RSW.

(4) Interfacial fracture occurs predominantly in the welded specimens. It is thought that this fracture results mainly from the high carbon equivalent of the welding materials and the presence of the sharp notch at the weld boundary. Furthermore, the presence of voids or cracks that are generated by solidification in the fractured surface would result in interfacial fracture. However, although interfacial fracture occurred in the specimen welded at a high current, the load-carrying capacity was still sufficiently high.

Acknowledgment

This research was financially supported by the Ministry of Knowledge Economy (MKE) and Korea Industrial Technology Foundation (KOTEF) through the Human Resource Training Project for Strategic Technology and the National Research Foundation of Korea Grant funded by the Korean Government (NRF-2009-K20601000004-09E0100-00410).

Nomenclature

Q : Heat input (J)
I : Weld current (A)
R : Resistance (Ω)
t : Weld time (s)
T : Thickness of thinner sheet of two plates (mm)

References

[1] POSCO Co., LTD., *Automotive Steel Data Book*, Copylight by POSCO, Korea (2008).

[2] J. H. An, D. C. Ko, C. J. Lee and B. M. Kim, Springback compensation of sheet metal bending process based on DOE and ANN, *J. Korean Society of Mechanical Engineering A*, 32 (11) (2008) 905-1046.

[3] C. J. Lee, J. Y. Kim, S. K. Lee, D. C. Ko and B. M. Kim, Parametric study on mechanical clinching process for joining aluminum alloy and high strength steel sheets, *J. of Mechanical Science and Technology*, 24 (2010) 123-126.

[4] L. Vaissiere, J. P. Laurent and A. Reinhardt, Development of pre-coated boron steel for applications on PSA Peugeot Citroën and RENAULT bodies in White, *SAE Paper*, No. 2002-01-2048 (2002).

[5] M. Merklein and J. Lechler, Determination of material and process characteristics for hot stamping processes of quenchenable ultra high strength steels with respect to a FE-based process design, *SAE Paper*, No. 2008-01-0853 (2008).

[6] X. Sun, E. V. Stephens and M. A. Khaleel, Effect of fusion zone size and failure mode on peak load and energy absorption of advanced high strength steel spot welds under lap shear loading conditions, *Engineering Failure Analysis*, 15 (2008) 356-367.

[7] S. S. Park, Y. M. Choi, D. G. Nam, Y. S. Kim, J. H. Yu and Y. D. Park, Evaluation of resistance spot weld interfacial fractures in tensile-shear tests of TRIP1180 steels, *J. Korean Welding and Joining Society*, 26 (6) (2008) 625-635.

[8] M. Milititsky and E. Pakalnines, On characteristics of DP600 resistance spot welds, *SAE Paper*, No. 2003-01-0520 (2003).
[9] J. Y. Baek, J. G. Lee and S. H. Rhee, A study of dynamic characteristics for resistance spot welding process using servo-gun system, *J. Korean Welding and Joining Society*, 23 (3) (2005) 40-46.
[10] H. W. Lee, Y. H. Kim, S. H. Lee, S. K. Lee, K. H. Lee, J. U. Park and J. H. Sung, Effect of boron contents on weldability in high strength steel, *J. of Mechanical Science and Technology*, 21 (2007) 771-777.
[11] J. H. Cha, A study on resistance spot weldability of aluminum coated sheet steels, Master's Thesis, *Pukyong National University* (2002).
[12] C. Ma, D. L. Chen, S. D. Bhole, G. Boudreau, A. Lee and E. Biro, Microstructure and fracture characteristics of spot-welded DP600 steel, *Materials Science and Engineering A*, 485 (2008) 334-346.
[13] G. E. Totten, Steel Heat Treatment-Metallurgy and Technology, Taylor and Francis, New York, USA (2006) 193-196.
[14] H. S. Choi, G. H. Park, W. S. Lim, S. B. Lee and B. M. Kim, The Optimization of Resistance Spot Weld Condition of Single Lap Joint for 22MnB5 Considering Heating Temperature and Heating Time in the Hot Stamping Process, *J. Korean Society of Mechanical Engineering A*, 34 (10) (2010).
[15] KS B 0851, Specimen dimensions and procedure for shear testing resistance spot and embossed projection welded joints (2006).
[16] KS B 0850, Method of inspection for spot weld (2006).
[17] M. Marya and X. Q. Gayden, Development of requirements for resistance spot welding dual-phase (DP600) steels; Part 1-The causes of interfacial fracture, *Welding Journal*, 84 (2005) 172-182.
[18] M. I. Khan, M. L. Kunts, E. Biro and Y. Zhou, Microstructure and mechanical properties of resistance spot welded advanced high strength steels, *Materials Transaction*, 49 (7) (2008) 1629-1637.
[19] X. Liao, X. Wang, Z. Guo, M. Wang, Y. Wu and Y. Rong, Microstructures in a resistance spot welded high strength dual phase steel, *Material characterization*, 61 (2010) 341-346.

Hong-Seok Choi is currently a Ph. D candidate at the Precision Manufacturing Systems Division at Pusan National University in Busan, Korea. His current research interests include hot sheet metal forming.

Byung-Min Kim received his B.S., M.S. and Ph. D. degrees from Pusan National University, Korea, in 1979, 1984 and 1987, respectively. He is currently a professor at the School of Mechanical Engineering at Pusan National University in Busan, Korea.